Calculation of the bonding strength of semi-crystalline polymers during overmolding

Anna Héri-Szuchács [a,b], József Gábor Kovács [a,b,*]

[a] Department of Polymer Engineering, Faculty of Mechanical Engineering, Budapest University of Technology and Economics, Műegyetem rkp. 3., H-1111, Budapest, Hungary
[b] MTA-BME Lendület Lightweight Polymer Composites Research Group, Műegyetem rkp. 3., H-1111, Budapest, Hungary

ARTICLE INFO

ABSTRACT

Injection molding is widely used in the plastics manufacturing industry. However, there is a need to better understand and calculate the bonding strength between the injection-molded part and the insert, especially for semi-crystalline polymers. The weldability of semi-crystalline polymers differs from that of amorphous polymers. Semi-crystalline polymers cannot heal until they reach their glass transition temperature, unlike amorphous polymers, as the crystalline particles prevent molecule motion below this temperature. To account for this difference, we have developed a method that takes into effect the crystalline parts of semi-crystalline polymers in the calculation of healing. We used polypropylene (PP) in our experiments, and calculated healing with a new method based on the method we previously described for the healing of amorphous polymers.

1. Introduction

Nowadays, more and more hybrid technologies are used, which combine two or more technologies to produce a product [1,2]. Hybrid technologies can improve the performance and appearance of the product, and extend design freedom [3–5]. One of the most common hybrid technologies is injection overmolding, where the polymer is injection molded onto a previously produced part. Although overmolding is a widespread technology, achieving a proper weld between the insert and the overmolded part is challenging [6], as bond strength depends on many factors [7]. Nowadays, a lot of simulation software is available to model injection molding, including overmolding [8–10], but none can calculate the strength of the weld created during overmolding.

Theories for calculating the healing of thermoplastic polymers can be found in the literature. Most of these theories are based on the theory of reptation presented by de Gennes [11], which describes the movement of macromolecules in a thermoplastic polymer melt. This theory models the macromolecule as being in an imaginary tube. When the temperature rises above a certain level, the molecule starts to leave this imaginary tube. The time it takes for the macromolecule to leave the tube completely is called reptation time. This is the time required for the polymer to fully heal at a given temperature and for its properties to match those of the bulk material [11].

The theory of reptation has been successfully applied to weld lines [12], the welding of polymer films [13], fusion bonding [14], and Automated Fiber Placement and Automated Tape Placement [15].

The reptation theory can only be used directly for isothermal processes, but several researchers have published formulas that can be used for non-isothermal processes. Among these, the most widely used are the Bastien and Gillespie [14], the Somnez and Hahn [16], and the Yang and Pitchumani models [17]. Previous research has shown that the Yang and Pitchumani formula can be applied the most accurately to calculate the degree of healing during the injection overmolding of amorphous materials (D_h), using the reptation time and taking into account the unequal temperature distribution during injection molding (Equation (1)) [2].

$$D_h = \frac{\sigma}{\sigma_\infty} = \left[\int_0^t \frac{1}{t_R(T)} dt \right]^{\frac{1}{4}} \tag{1}$$

where t_R is the reptation time, σ is actual bond strength, and σ_∞ is ultimate bond strength.

The healing of semi-crystalline and amorphous materials differs in that macro-Brown motion is required for healing. For semi-crystalline polymers, the macro-Brown motion stops when the crystallization

Table 1

Material properties for the polypropylenes.

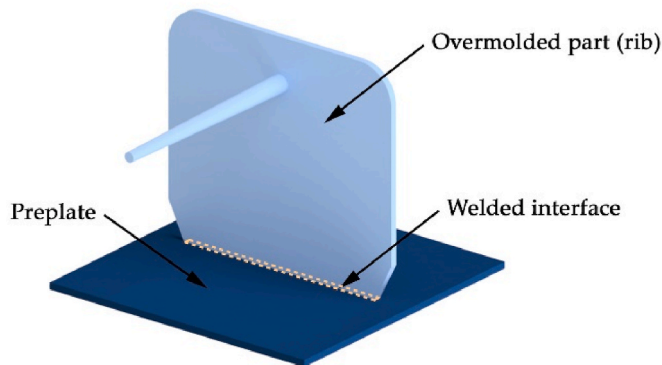| Material	Tm [°C]	Tg [°C]	MFR [g/10 min]	C2 content [m%]
H145F	163.9	−4.6	29	0
R959A	148.4	−12.6	45	3–5

Fig. 1. T-shape specimen used for the examination of bonding strength.

temperature range is reached, whereas amorphous polymers continue until the glass transition temperature is reached. This is because the crystalline regions hinder the movement of molecules [18]. Several studies have addressed the healing of semi-crystalline materials. Akkerman et al. [19] developed a method to account for crystalline regions. Their method assumes that the degree of healing is equal to the degree of melting at the maximum temperature reached during injection molding. Their results showed that the calculation can only characteristically describe the degree of melting. Guisti and Lucchetta [20] used a polypropylene material for their experiments and used Bastien's formula to calculate the bond strength of injection overmolded semi-crystalline polymers. Their calculation had a significant error, in some cases more than 30 %.

While in amorphous materials, healing is slow at the beginning of the range of healing and increases with increasing temperature, in semi-crystalline polymers, healing is very fast at the beginning of the range of healing, especially near the melting temperature range [21–23]. Therefore, it is crucial to define limit temperatures when healing starts and stops to calculate the degree of healing accurately. In their study, Guisti and Luchetta [24] used the no-flow temperature as the limit temperature, and Yang and Pitchumani [17] used the melting temperature measured by DSC.

In this paper, we calculate the healing of semi-crystalline polymers using our previously described calculation method for amorphous polymers and present a suitable method to determine the limit temperatures when healing starts and stops.

2. Materials and methods

2.1. Materials

We used two different polypropylenes. One of the materials we used was a homopolymer (MOL Tipplen H145F), and the other was a random copolymer (MOL Tipplen R959A) (Table 1).

2.2. Preparation of samples

2.2.1. Production of specimens

A ″T-shaped specimen″ was used for the tensile test. This specimen comprises an 80 mm × 80 mm x 2 mm base plate and a 70 mm × 63 mm x 2 mm overmolded rib. Bond strength can be assessed in the weld area between the two components, which has a nominal size of 60 mm × 2

Table 2

Process parameters used for injection overmolding.

Melt temperature (°C)	190/210/230/250
Cooling water temperature (°C)	40
Waiting time before injection (s)	5
Injection rate (cm³/s)	30
Switchover, pressure on the sensor (bar)	50
Holding pressure (−)	80 % of injection pressure
Holding time (s)	7
Cooling time (s)	20

mm (see Fig. 1). We conducted the test at four different temperatures to determine the effect of melt temperature on weld strength. The manufacturing parameters for overmolding are detailed in Table 2. Switchover was controlled by pressure, via a Cavity Eye RC15 pressure sensor (Cavity Eye Hungary Kft, Kecskemét, Hungary). In each set, ten test specimens were produced. The base plate was created with an Arburg Allrounder Advance 270S 400-170 (ARBURG GmbH Germany, Lossburg) injection molding machine, and the rib was overmolded with an Arburg Allrounder 470 A 1000-290 (ARBURG GmbH Germany, Lossburg) injection molding machine.

Single-piece specimens were produced at all temperatures with identical process parameters. In this case, the base plate was not inserted into the mold, so the entire specimen was produced in one cycle and thus had no weld surface. The strength of these specimens was used to calculate the bond strength of overmolded specimens.

2.2.2. Mechanical testing

The bond strength of the specimens was tested with a universal Zwick Z020 tensile testing machine (Zwick Roell AG, Ulm, Germany) with a 20 kN load cell and a crosshead speed of 5 mm/min. We employed a grip we specially designed for the tensile test because existing grips cannot be used for these specimens. Our grip enabled precise measurements of material strength, ensuring reliable results for the T-shape specimens [2].

2.2.3. Results

The bond strength of both polypropylenes increased significantly with increasing melt temperature. The homopolymer (H145F) had a lower bond strength under the same conditions (Fig. 2/a), even though the tensile strength of this material is much higher than that of the random copolymer (R959A) (Fig. 2/b). These results indicate that the homopolymer has worse welding properties than the random copolymer tested.

2.3. Characterization

2.3.1. Rheological testing

To calculate the reptation time of the materials, we performed frequency sweep tests with a parallel plate rotational rheometer AR2000 (TA Instruments, New Castle, USA). We calculated the reptation time from the reciprocal of the first crossover frequency of the elastic modulus (G′) and storage modulus (G″) (Equation (2)), using a simplification, as commonly used in the literature.

$$t_R(T) = \frac{1}{\omega_{1X}(T)} \tag{2}$$

A shear strain of 0.5 % was used in the test, and the diameter of the tested plates was 25 mm. Reptation time was measured at five temperatures (180, 200, 220, 240, and 260 °C), then the WLF curve was fitted to the measured values (Equation (3)) (Table 3).

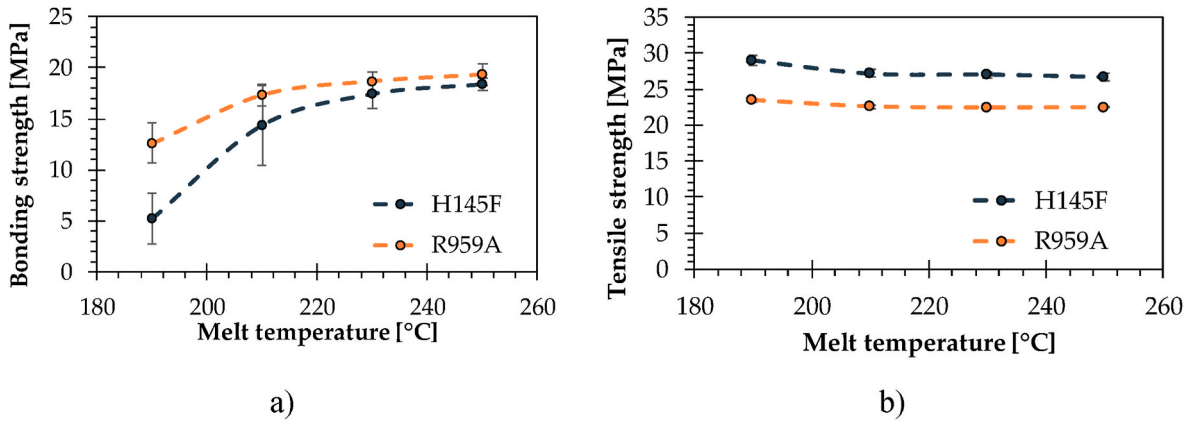$$\log a_T = \log \frac{t_R(T)}{t_{R,ref}} = \frac{C_1 (T - T_{ref})}{C_2 + (T - T_{ref})} \tag{3}$$

Fig. 2. The measured tensile strength of a) overmolded specimens and b) single-piece specimens.

Table 3
Fitted WLF constants for the polypropylenes used.

Material	H145F	R959A
C_1 [-]	2.20	2.21
C_2 [°C]	190	190
T_{ref} [°C]	170	170
t_{Rref} [s]	0.0075	0.0023984

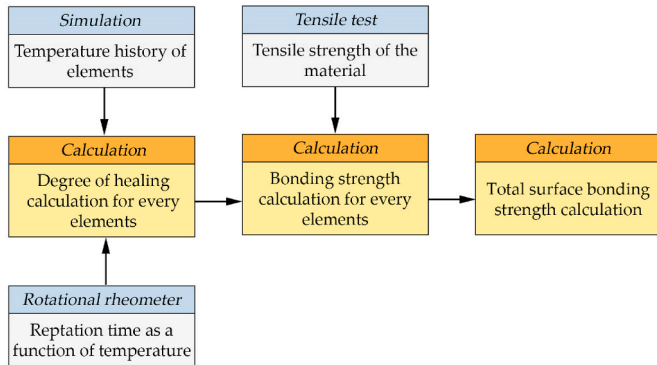**Fig. 3.** Steps of the bonding strength calculation method and the data required for the steps.

2.3.2. Thermal testing

We performed flash DSC tests to investigate the crystallization properties of the materials. Several cooling and heating rates were used in the tests.

2.4. Simulation

The temperature history of the contact surface was determined with the use of the Moldex3D R21 (CoreTech System Co. Hsinchu, Taiwan) simulation; the process parameters were the same as in injection overmolding.

3. Calculation and results

3.1. Calculation for amorphous polymers

We have developed a calculation method to determine the bonding strength of amorphous polymers (Fig. 3). The initial step is calculating the degree of healing (Dh) for all surface elements. The modified Yang formula (Equation (4)) can be employed to calculate the degree of healing, which makes it necessary to calculate the reptation time(t_R(T))
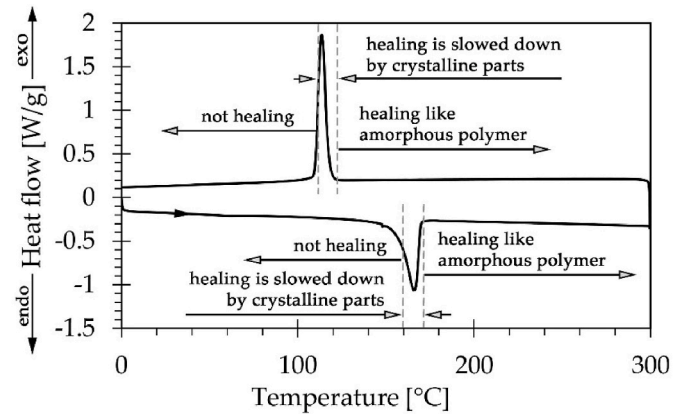

Fig. 4. The bonding of semi-crystalline polymers demonstrated with their DSC curve.

for each element, which can be obtained from the simulated temperature history with the use of the WLF equation (Section 2.2.3) (Equation (3)).

$$D_h = \left[\int_o^t \frac{1}{t_R(T)} dt \right]^{1/4} \tag{4}$$

where

$$t_R(T) = 10^{\frac{C_1(T-T_{ref})}{C_2+(T-T_{ref})}} * t_{R,ref} \tag{5}$$

From the degree of healing for each element, the bond strength of the element can be determined with the use of the tensile strength of the material (Equation (6)). For this purpose, we used the tensile strength of the injection-molded pieces in our experiments.

$$\sigma = D_h * \sigma_\infty \tag{6}$$

We can obtain a weld distribution map for the overmolded surface with the bonding strengths calculated this way. For validation, however, we need the bond strength of the entire surface, which can be measured with a tensile test. This can be determined by tensile test modeling from the bond strength of the elements, which was discussed in detail in our previous paper [1].

3.2. The difference between the healing of amorphous and semi-crystalline polymers

The method with which the bonding strength of amorphous polymers was calculated cannot be used directly with semi-crystalline
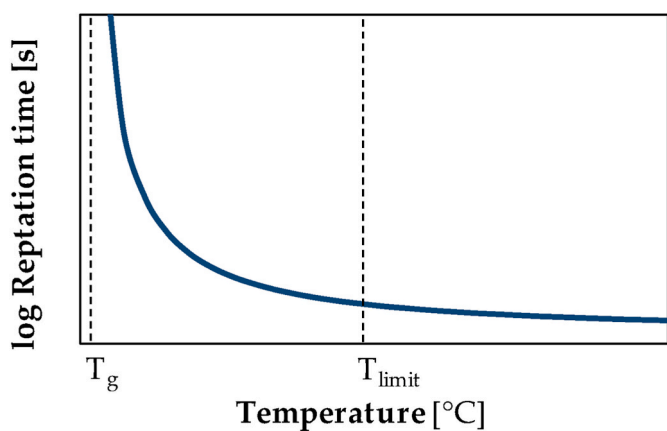
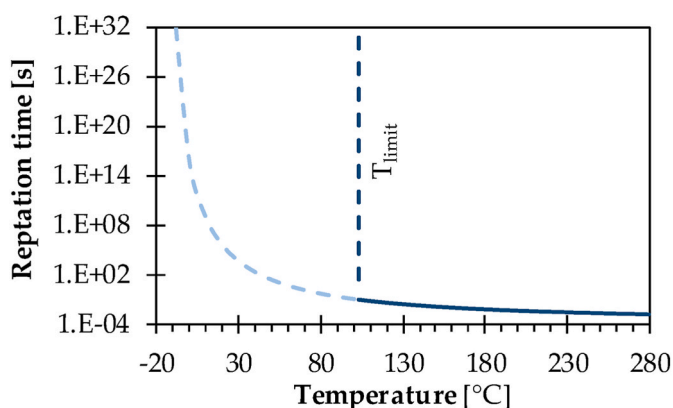**Fig. 5.** Fitted WLF curve as a function of temperature.

Fig. 6. Defined reptation time curve for semi-crystalline polymers.

Fig. 7. Flash DSC results of MOL Tipplen H145F in the case of cooling.

Fig. 8. Flash DSC results of MOL Tipplen H145F in the case of heating.

Fig. 9. The chosen limit temperature (with blue) and the start and end of the crystallization temperature range as a function of cooling and heating rate for MOL Tipplen H145F. (For interpretation of the references to colour in this figure legend, the reader is referred to the Web version of this article.)

polymers since the crystalline regions strongly influence the movement of the polymer molecules. However, in the melt state, the crystalline parts break up, and the whole material is in the amorphous phase. Therefore, the calculation method described for amorphous polymers can be applied to semi-crystalline materials above the crystal melting temperature. At the beginning of the formation of crystalline regions, the movement of the molecules is only slightly restricted. Then, as the number and size of crystalline regions increase, the movement of the molecules becomes more and more restricted until the molecules can no longer diffuse, and thus, the bonding process stops (Fig. 4).

We aimed to describe the effect of crystalline regions using the reptation time curve and thus make the calculation method for amorphous polymers applicable to semi-crystalline polymers.

The reptation time curve varies with temperature and can be described with the WLF equation. The motion of the molecular chains of amorphous polymers stops at the glass transition temperature so the material cannot heal below this temperature. Consequently, the reptation time at the glass transition temperature is infinite, which can be seen from a properly fitted WLF curve (Fig. 5).

Similarly to amorphous polymers, the reptation time of semi-crystalline polymers is also infinite at the glass transition temperature. The molecule would have sufficient energy for motion up to the glass transition temperature. To consider the limiting effect of crystallization, we defined a limit temperature at which healing stops. The formation of crystalline regions does not occur at a specific temperature but over a range of temperatures, since the cooling rate during injection molding is very high (about 500–1000 °C/min), so the formation of crystalline regions can be considered instantaneous. Therefore, we simplified the process by assuming that the healing of semi-crystalline polymers stops
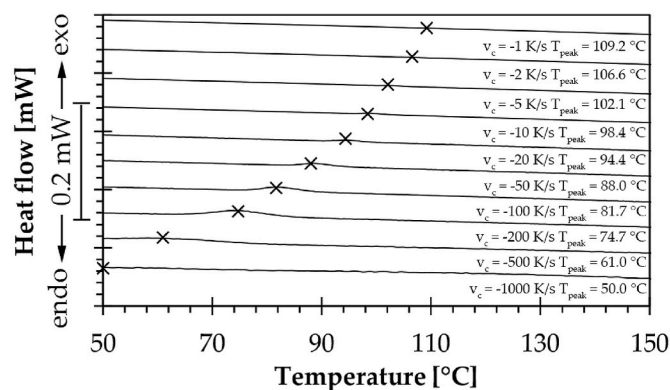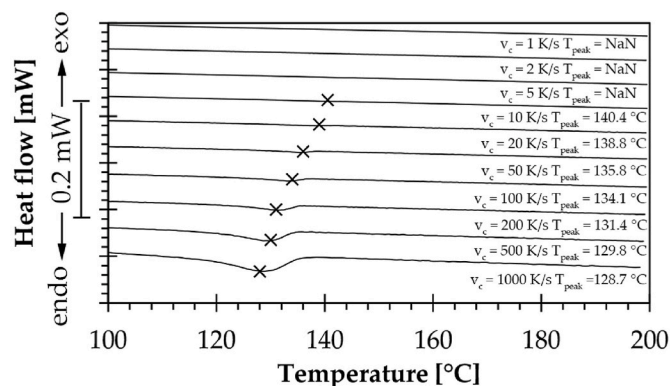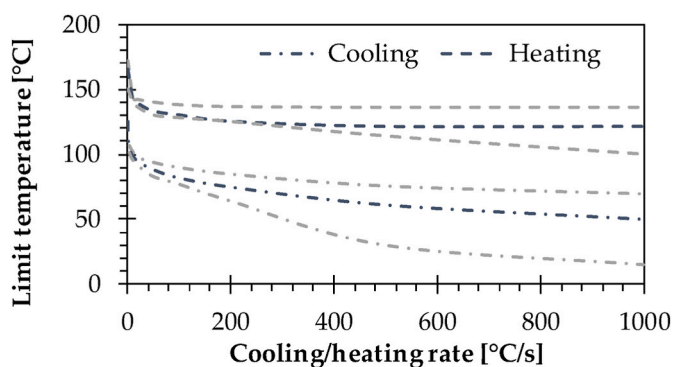
at a specific temperature, which we called the limit temperature. At the limit temperature, the healing of the polymer stops, therefore the modified shift factor and the reptation time increase to infinity (Fig. 6).

3.3. Determining the limit temperature

To determine the limit temperature, we have to investigate the crystallization properties of the polymer. Since the crystallization temperature range of polymers greatly depends on the cooling rate and cooling rates are high during injection molding, we measured the crystallization temperature range of the materials at different cooling rates using Flash DSC (Fig. 7). The limit temperature was determined for
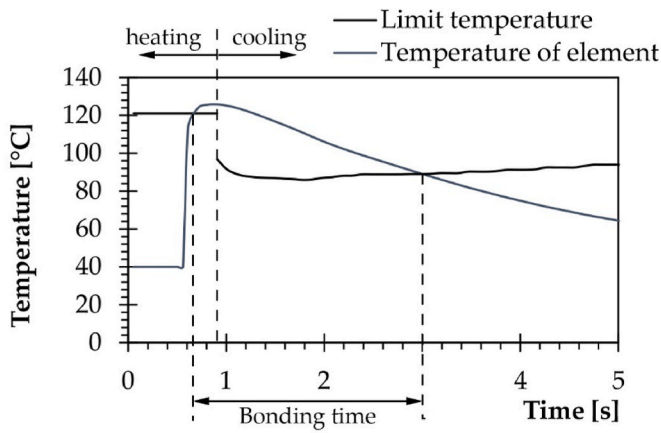
Fig. 10. The limit temperature calculated from the temperature history of an element on a healing surface and the bonding interval.
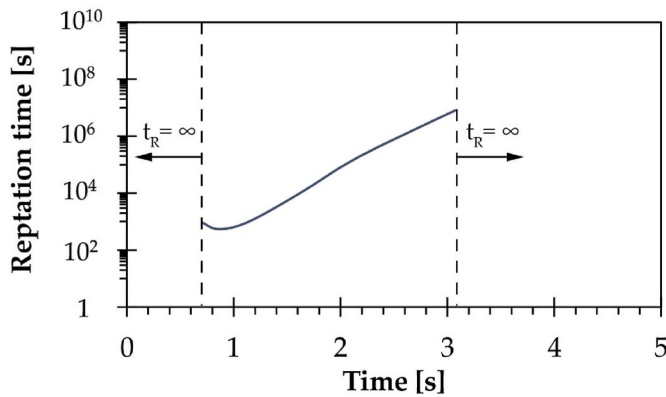

Fig. 11. Example of a reptation time curve of an element with a temperature history shown in Fig. 10 for a semi-crystalline polymer (MOL Tipplen H145F) – the curve is similar for other semi-crystalline polymers.

each cooling rate within the crystallization temperature range measured with that cooling rate.

In the injection molding process, the inserts heat up. For an accurate detection of the onset of healing, it is necessary to establish a limit temperature curve based on the heating rate. This requires determining the melting temperature of the polymer, which we did with Flash DSC tests at varying heating rates (Fig. 8).

With Flash DSC, the start and end of the crystallization temperature range can be identified based on the applied cooling and heating rate (Fig. 9). Within this temperature range, the limit temperature for healing is determined. Its value can be affected by various factors such as the crystalline proportion and the type of crystals.

3.4. Reptation time curve of semi-crystalline polymers

Once the limit temperature curve for the material has been determined, the first step in the calculation is to determine the reptation time curve. To determine the reptation time curve, we have to determine the limits of healing. For that, the first step is to determine the cooling and heating rates from the modeled temperature history of a given point on the healing surface. Fig. 10 shows how the cooling and heating limit temperatures can be determined.

Healing starts when the temperature of the point is heated above the heating limit temperature and continues until the temperature of the point falls below the cooling limit temperature. Between these two points, the reptation time can be calculated from the fitted WLF equation determined with the rotational rheometer. In contrast, the reptation time outside this interval is infinite since no healing occurs (Fig. 11). From reptation time curves calculated in this way, the bonding strength of the whole surface can be calculated with our calculation method (Section 3.1) [1].

3.5. Validation

The method was validated with two types of polypropylene. We observed that the calculation method provides accurate estimates of the measured bonding strengths when appropriate limit temperatures are selected (Fig. 12). The calculated bonding strengths for both materials fall within the standard deviation of measured bonding strengths, except at the maximum melt temperature for the homopolymer and at the minimum melt temperature for the random copolymer. In both these cases, calculated bonding strength overestimates actual bonding strength.

4. Conclusion

This article details our effective bonding strength calculation method for semi-crystalline materials. To develop this method, we built upon our existing calculation technique designed for amorphous polymers and made necessary adjustments. Our approach involves creating a limit temperature curve, which accurately determines the beginning and end of the healing process in semi-crystalline polymers. To validate our method, we tested two distinct types of polypropylenes: a homopolymer and a random copolymer. Our findings indicate that our calculation
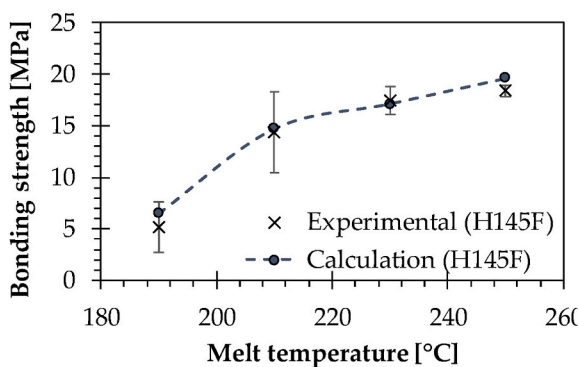
a)
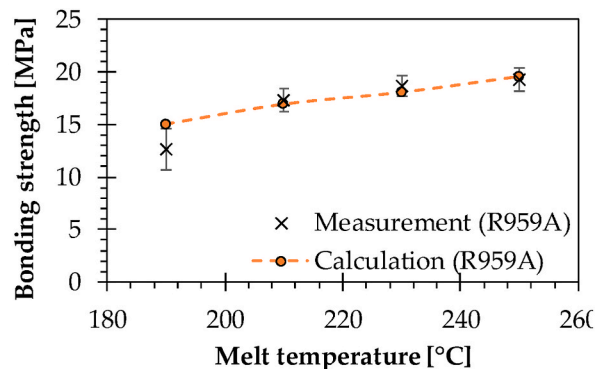
b)

Fig. 12. Measured and calculated bonding strength of a) a homopolymer polypropylene (MOL Tipplen H145F) and b) a random copolymer polypropylene (MOL Tipplen R959A).

method can predict bonding strength with high accuracy, with an average error rate of under 10 %.

Funding

Data availability statement

The data that support the findings of this study are available from the corresponding author upon reasonable request.

CRediT authorship contribution statement

Anna Héri-Szuchács: Writing – original draft, Validation, Software, Methodology, Conceptualization. **József Gábor Kovács:** Writing – review & editing, Validation, Supervision, Resources, Methodology, Funding acquisition, Conceptualization.

Declaration of competing interest

The authors declare that they have no known competing financial interests or personal relationships that could have appeared to influence the work reported in this paper.

Acknowledgments

References

[1] A. Szuchács, T. Ageyeva, J.G. Kovacs, Modeling and Measuring the Bonding Strength of Overmolded Polymer Parts Polymer Testing, vol. 125, 2023 108133, https://doi.org/10.1016/j.polymertesting.2023.108133. ISSN 0142-9418.

[2] A. Szuchács, T. Ageyeva, R. Boros, J.G. Kovacs, Bonding strength calculation in multicomponent plastic processing technologies, Mater. Manuf. Process. 36 (2021) 1–9, https://doi.org/10.1080/10426914.2021.1948052.

[3] M.Z. Huang, J. Nomai, A.K. Schlarb, The effect of different processing, injection molding (IM) and fused deposition modeling (FDM), on the environmental stress cracking (ESC) behavior of filled and unfilled polycarbonate (pc), Expreess Polymer Letters 15 (2021) 194–202, https://doi.org/10.3144/expresspolymlett.2021.18.

[4] T. Schneider, Lightweight construction: first composite gearbox housing with layeroptimized organo sheeting weighs 30% less than a comparable aluminum component, Reinforc Plast 63 (2019) 40–45, https://doi.org/10.1016/j.repl.2017.11.018.

[5] G. Gardiner, Camisma's car seat back: hybrid composite for high volume. https://www.compositesworld.com/articles/camismas-car-seat-back-hybrid-composite-for-high-volume. (Accessed 21 January 2020).

[6] L. Pisanu, J. Barbosa, P. Bamberg, B. Marx, A. Schiebahn, R. Souza, M. Nascimento, Influence of coupling agents on the adhesion force of dissimilar overmolded polymers: a digital image correlation analysis, Materia 24 (2019), https://doi.org/10.1590/s1517-707620190003.0800.

[7] T. Geminger, S. Jarka, 4 - injection molding of multimaterial systems, in: H.-P. Heim (Ed.), Specialized Injection Molding Techniques, William Andrew Publishing, 2016, https://doi.org/10.1016/B978-0-323-34100-4.00004-3pp165-210.

[8] M.-L. Wang, R.-Y. Chang, C.-H. Hsu, 5 - molding simulation methodology, in: M.-L. Wang, R.-Y. Chang, C.-H. Hsu (Eds.), Molding Simulation: Theory and Practice, Hanser, Munich, 2018, pp. 123–158, https://doi.org/10.3139/9781569906200.005pp.

[9] M.-W. Wang, F. Arifin, V.-H. Vu, The study of optimal molding of a LED lens with grey relational analysis and molding simulation, Period. Polytech. - Mech. Eng. 63 (4) (2019) 278–294, https://doi.org/10.3311/PPme.13337.

[10] A. Benayad, R. El Otmani, A. El Hakimi, M. Boutaous, A. Touache, R.K. Musa, S. Derdouri, N. Mahfoudi, D. Siginer, Experimental investigation and numerical simulation of the microinjection molding process through an expanding flow configuration, Pol. Adv. Tech (2021) 1–22, https://doi.org/10.1002/pat.5206.

[11] P.G. de Gennes, Reptation of a polymer chain in the presence of fixed obstacles, J. Chem. Phys. 55 (2) (1971) 572, https://doi.org/10.1063/1.1675789.

[12] C.A. Cruz, Integrative simulation for assessing the mechanical performance of a weld line on injection moulded thermoplastic parts, in: Proceedings of 11th World Congress on Computational Mechanics (WCCM XI), 5th European Conference on Computational Mechanics (ECCM V) and 6th European Conference on Computational Fluid Dynamics (ECFD VI), 2014. Barcelona, Spain, 20-25 July.

[13] D. Grewell, A. Benatar, Semi-empirical, squeeze flow and intermolecular diffusion model I. Determination of model parameters, Pol. Eng. & Sci. 48 (2008) 860–867, https://doi.org/10.1002/pen.21021.

[14] L.J. Bastien, J.W. Gillespie, A non-isothermal healing model for strength and toughness of fusion bonded joints of amorphous thermoplastics, Polym. Eng. Sci. 31 (24) (1991) 1720–1730, https://doi.org/10.1002/pen.760312406.

[15] K. Yassin, M. Hojjati, Processing of thermoplastic matrix Composites through automated fiber placement and Tape laying methods: a review, J. Thermoplastic Comp. Mat. 3112 (2018) 1676–1725, https://doi.org/10.1177/0892705717738305.

[16] F.O. Sonmez, H.T. Hahn, Analysis of the on-line consolidation process in thermoplastic composite Tape placement, J. Thermoplastic Comp. Mat. 10 (6) (1997) 543–572, https://doi.org/10.1177/089270579701000604.

[17] F. Yang, R. Pitchumani, Healing of thermoplastic polymers at an interface under nonisothermal conditions, Macromolecules 35 (8) (2002) 3213–3224, https://doi.org/10.1021/ma010858o.

[18] Y.M. Boiko, G. Guerin, V.A. Marikhin, R.E. Prud'homme, Healing of Interfaces of Amorphous and Semi-crystalline Poly(ethylene Terephthalate) in the Vicinity of the Glass Transition Temperature, 2001.

[19] R. Akkerman, M. Bouman, S. Wijskamp, Analysis of the Thermoplastic Composite Overmolding Process: Interface Strength, Frontier in Materials, vol. 7, 2020, https://doi.org/10.3389/fmats.2020.00027.

[20] R. Giusti, G. Lucchetta, Modeling the adhesion bonding strength in injection overmolding of polypropylene parts, Polymers 12 (2020) 2063, https://doi.org/10.3390/polym12092063.

[21] G.D. Smith, C.J. Plummer, P.E. Bourban, J.A.E. Manson, Non-isothermal fusion bonding of polypropylene, Polymer 42 (2001) 6247–6257, https://doi.org/10.1016/S0032-3861(01)00060-X.

[22] J.E. Zanetto, C.J. Plummer, P.E. Bourban, J.A.E. Manson, Fusion bonding of polyamide 12, Polym.Eng.Sci. 41 (2001) 890–897, https://doi.org/10.1002/pen.10787.

[23] C.J. Plummer, P.E. Bourban, J.E. Zanetto, G.D. Smith, J.A.E. Manson, Nonisothermal fusion bonding in semicrystalline thermoplastics, Applied Polymer Science 87 (2002), https://doi.org/10.1002/app.11528.

[24] R. Giusti, G. Lucchetta, Modeling the adhesion bonding mechanism in overmolding hybrid structural parts for lightweight applications, Key Eng. Mater. 611–612 (2014) 915–921. https://doi.org/10.4028/www.scientific.net/KEM.611-612.915.